Revista Brasileira de Recursos Hídricos
Brazilian Journal of Water Resources
Versão On-line ISSN 2318-0331
RBRH, Porto Alegre, v. 30, e21, 2025
Scientific/Technical Article

https://doi.org/10.1590/2318-0331.302520250009

The influence of topography on floods in southern Brazil

A influência da topografia nas inundações do extremo sul do Brasil

Vinícius Kuchinski[1] & Rodrigo Cauduro Dias de Paiva[1]

[1]Instituto de Pesquisas Hidráulicas, Universidade Federal do Rio Grande do Sul, Porto Alegre, RS, Brasil
E-mails: kuchinski@outlook.com (VK), rodrigo.paiva@ufrgs.br (RCDP)

Received: January 14, 2025 - Revised: February 22, 2025 - Accepted: March 08, 2025

ABSTRACT

Understanding the characteristics of watersheds is fundamental for hydrological studies. This study investigates the influence of topographic and hydrological features in watersheds located in the extreme south of Brazil about flood events, which are recurrent in the region. Watersheds were classified based on their exposure to flooding, and differences in their characteristics were analyzed and compared. The results indicate that greater watersheds, with larger area, perimeter, and drainage network, are more exposed to flooding. These watersheds exhibit a floodplain relief profile resembling a "U" shape and possess a larger floodable area, in contrast to less exposed watersheds, which display a "V"-shaped relief profile. Furthermore, the specific discharge values of the more exposed to flooding watersheds are lower than those of the less exposed watersheds, suggesting that the larger floodplain area may contribute to flood attenuation. These findings offer valuable insights for preliminary watershed management and flood risk assessment.

Keywords: Flood susceptibility; Morphometric analysis; Floodplain; Watershed.

RESUMO

O conhecimento da bacia hidrográfica é fundamental para estudos hidrológicos. Esse trabalho investiga a influência de características topográficas e hidrológicas em bacias do extremo sul do Brasil sobre os eventos de inundação, que são recorrentes na região. As bacias foram separadas de acordo com a sua exposição a inundações e as diferenças de suas características foram avaliadas e comparadas. Os resultados indicam que bacias mais largas, com maior área, perímetro e drenagem são mais expostas a inundação, com perfil de relevo na planície de inundação mais próximo do formato da letra "U" e maior área inundável, diferente das bacias menos expostas, com um relevo mais próximo do formato da letra "V". Além disso, as vazões específicas das bacias mais expostas têm valores menores que as das bacias menos expostas, indicando uma possível atenuação das cheias pela planície de inundação. Essas descobertas colaboram com o gerenciamento preliminar de bacias hidrográficas e avaliação de risco de inundações.

Palavras-chave: Suscetibilidade a inundações; Análise morfométrica; Planície de inundação; Bacia hidrográfica.

INTRODUCTION

Flood events are among the most devastating natural disasters globally, posing significant threats to human populations (Blöschl, 2022). Understanding river flooding and its associated impacts are critical for reducing risks (Merz et al., 2021). In this context, watersheds serve as fundamental units for studying hydrological events (Nasir et al., 2020).

A comprehensive focus on various aspects of watersheds, including morphometry, geological characteristics, and land use, is essential for effective water resources management (Alqahtani & Qaddah, 2019). Geospatial tools, such as remote sensing and geographic information systems (GIS), have been increasingly applied in watershed management (Sutradhar & Mondal, 2023). Advances in technology have also made high-resolution digital elevation models more accessible, enhancing the precision of watershed analysis (Obeidat et al., 2021) and enabling a detailed understanding of fluvial geomorphological processes (van Appledorn et al*.,* 2019).

Despite the accumulated knowledge about terrestrial hydrology, the role of topography in shaping the water cycle remains a complex and visible factor, continuing to puzzle and surprise researchers (Gnann et al., 2025). Morphological characteristics of watersheds have been studied for decades, with foundational works of Horton (1932, 1945) setting the stage for modern research. Current studies focus on identifying areas susceptible to flooding (Tola & Shetty, 2022), understanding the hydrological behavior of sub-basins (Rana & Suryanarayana, 2021), developing flood risk maps (Bhat et al., 2019), and prioritizing areas for risk management (Obeidat et al., 2021). The integration of morphometric parameters and GIS has become increasingly common in flood analysis, underscoring the importance of watershed characteristics in understanding flood patterns (Basahi et al., 2016; Chaithong, 2022).

Another perspective on morphology studies examines how morphological differences in river valleys can influence flooding. In this context, van Appledorn et al. (2019) demonstrated that valley morphology has a greater impact on flood patterns, including their extent and duration, than basin size. Similarly, Devitt et al. (2023) analyzed population exposure to floods, revealing regional differences in settlement patterns in flood-prone areas, particularly in Europe and Asia.

In Brazil, however, studies on floods using morphometry remain incipient. Research has primarily focused on characterizing watersheds (Vale & Bordalo, 2020), assessing flood susceptibility (Ávila et al., 2017; Franco & Santo, 2015), or providing broader physical characterizations of these systems (Negri & Fill, 2023). Yet, there is still limited understanding of how specific morphological differences between watersheds influence flood patterns, particularly in regions with distinct hydrological and climatic conditions, such as southern Brazil.

In the extreme south of Brazil, especially in Rio Grande do Sul, flood events have been recurrent. In the past two years (2023 and 2024), three major flood events have caused significant devastation, with the most recent considered the largest natural disaster in the region's history (Collischonn et al., 2024; Marcuzzo et al., 2024). This disaster affected more than 90% of the state's municipalities, impacted nearly 900,000 people, and resulted in over 180 fatalities (G1, 2024; Reboita et al., 2024; Rio Grande do Sul, 2024). Furthermore, studies suggest that climate change is expected to increase the frequency and intensity of flood events in the region due to rising precipitation levels and soil moisture (Brêda et al., 2023; Chagas et al., 2022).

Given this context, the objective of this study is to analyze whether morphological parameters differ between watersheds that are more exposed to flooding and those that are less exposed, through an evaluation of runoff-generating processes. Additionally, the study investigates the morphology of river valleys in their floodplains and their behavior during flood events of varying magnitudes by analyzing historical flood occurrences. This research aims to enhance the understanding of hydrological processes and contribute to improved flood risk management strategies in the southern Brazil.

METHODOLOGY

Study area

The study area corresponds to the hydrological region of Rio Grande do Sul (RS), as represented in Figure 1. The region is located in southern Brazil and encompasses the state of Rio Grande do Sul as well as the areas forming its river basins. Consequently, the study area extends beyond state borders, including parts of Santa Catarina in Brazil, as well as portions of Uruguay and Argentina.

This area was chosen due its significant regional importance and is an area that recurrently is affected by flood events, as highlighted in studies by Menezes & Sccoti (2013) and Berte et al. (2022). Moreover, recent study by Brêda et al. (2023) has indicated that climate change is likely to intensify these challenges by increasing the region's annual maximum precipitation and soil moisture levels.

Within this region, 28 municipalities most exposed to flooding were identified (Figure 1) by combining the classifications from Berte et al. (2022) and Menezes & Sccoti (2013). In the study conducted by Menezes & Sccoti (2013), municipalities were classified based on the number of flood occurrences between 1980 and 2010. For the purposes of this, those categorized as having a very high probability of flooding were selected. Similarly, in the study by Berte et al. (2022), municipalities with the highest number of flood occurrences were chosen based on records from the Integrated Disaster Information System (S2iD) for the period 2003 to 2021.

These municipalities are distributed across the study area from east to west, with a concentration in the central and southern portions. This distribution aligns with the region's topography, where the northeastern areas are characterized by higher elevations, while the western and central portions are predominantly lower in elevation.

Data used

The hydrological data utilized in this analysis were sourced from the CAMELS-BR dataset (Chagas et al., 2020). Of the 61 gauge stations located within the study area, 56 were effectively used after a data quality assessment. This assessment involved checking for missing data within the period spanning 1980-2018.

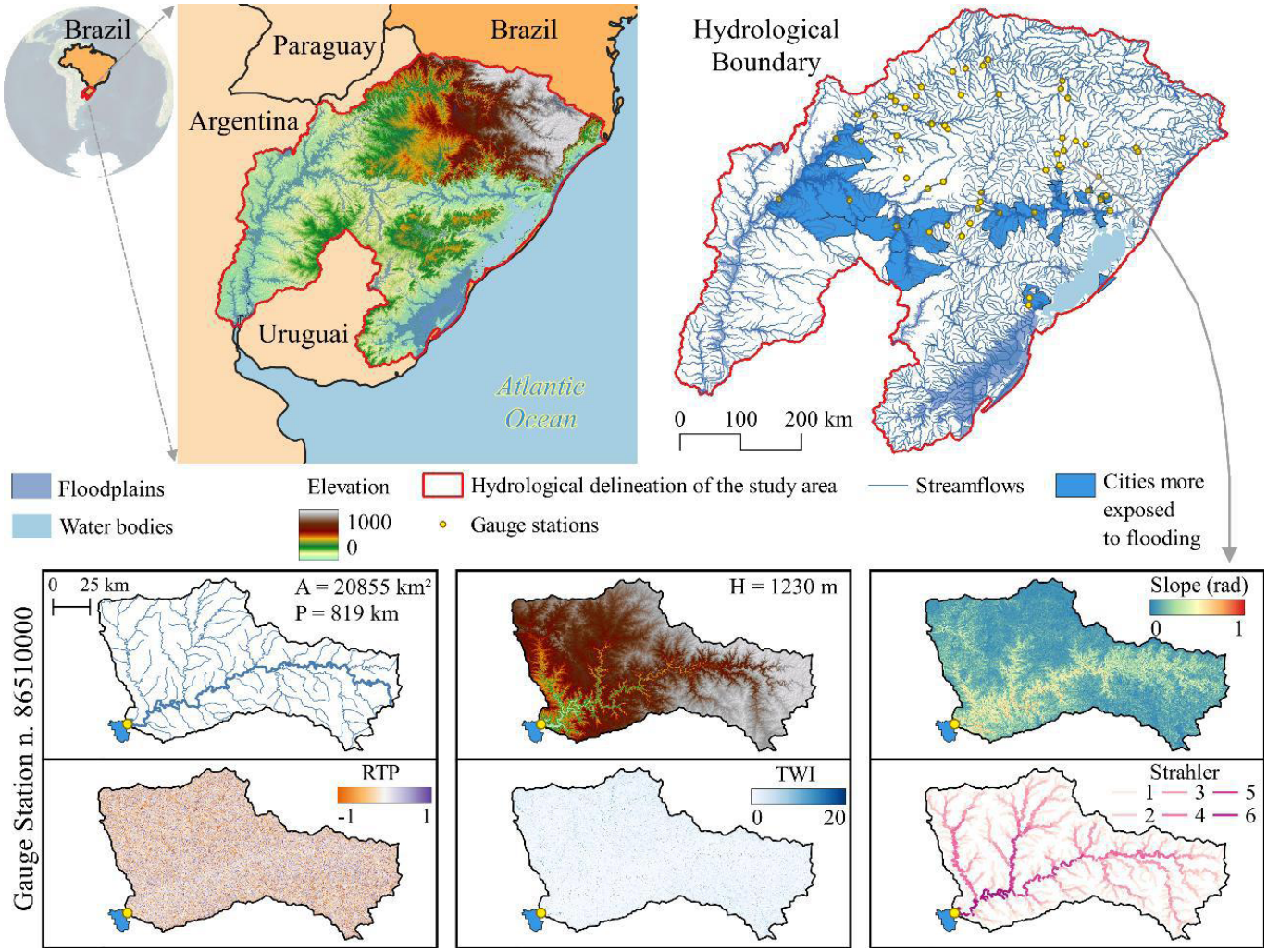

Figure 1. Top: Location of the study area — the hydrological region of Rio Grande do Sul — showing its boundaries, drainage network, and the streamflow gauge stations used in this study. Bottom: Selected morphometric parameters (e.g., gauge station n. 86510000, city of Muçum), including Relative Topographic Position (RTP) and Topographic Wetness Index (TWI).

Stations with incomplete records were excluded from the analysis. These stations are shown in Figure 1.

For the morphometric analysis, the digital elevation model (DEM) from the Shuttle Radar Topography Mission (SRTM) (Farr et al., 2007), with a spatial resolution of 90 meters, was employed. This elevation data facilitated the extraction of physical parameters for a complementary analysis, enabling comparisons of the characteristics of various watersheds within the study area. Examples of these parameters are shown in the lower portion of Figure 1, highlighting the gauge station located in the municipality of Muçum, which was severely affected by the flood events of 2023 and 2024.

All data analyses, as detailed in this section, were conducted using the Python programming language. When necessary, geoprocessing operations were performed using the open-source QGIS software. Links to respective data used and information about the gauge stations used are given in the Supplementary Material.

Morphometric relationships

The morphometric analysis of the watersheds in the RS was conducted using geoprocessing techniques and classical equations proposed by Horton (1945), Strahler (1952), and others. The attributes used in the analysis, their formulas, and references are summarized in Tables 1, 2 and 3. Most of these parameters are widely used in recent studies to compare basins (Chaithong, 2022), model flood susceptibility (Tola & Shetty, 2022), understand flood-related processes (Romshoo et al., 2012), and prioritize areas for flood risk assessment (Mahmoodi et al., (2023).

Below is the description of each linear parameter, summarized in Table 1:

- Stream order (S_u): Mainstream order, derived from Strahler's ranking (Strahler, 1952), measures the magnitude of the analyzed watercourse.
- Total stream number (N_u): A direct measure of the number of stream segments.
- Total stream length (L_u): A direct measure of the drainage network's extent.
- Mainstream length (L_{ms}): Measure of the main river's extent within the analyzed basin.
- Stream length ratio (R_l): The ratio between the lengths of segments of one order and the immediately lower order.

According to Horton (1945), it helps to understand the composition of the drainage system and serves as an indirect measure of discharge (Koralay & Kara, 2023).

- Mean stream length (L_{um}): An indirect measure of the extent of the basin's watercourses.
- Bifurcation ratio (R_b): The ratio between the number of segments of one order and the immediately higher order, aiding in understanding the drainage system's structure (Horton, 1945), and serves as an indirect measure of discharge (Dutal, 2023).
- Stream length/Bifurcation ratio (ρ): An indirect measure of the water storage capacity of the basin's drainage channels (Tola & Shetty, 2022).

Next, the description of each parameter related to area, summarized in Table 2:

- Basin area (A): A direct measure of the watershed area.
- Basin perimeter (P): A direct measure of the watershed perimeter.
- Drainage density (D_d): The ratio of the total stream length to the basin area, representing the drainage network's development (Horton, 1945).
- Stream frequency (F_s): The ratio of the number of stream segments to the basin area, which serves as an indirect measure of soil permeability (Koralay & Kara, 2023) or local flash flood susceptibility (Nasir et al., 2020).
- Texture ratio (R_t): The ratio of the number of stream segments to the basin perimeter, indicating the linear distance between stream segments that depends on various factors (Sutradhar & Mondal, 2023).
- Elongation ratio (R_e): The ratio between the diameter of a circular basin with the same area as the analyzed basin and its maximum length, indirectly indicating the basin's shape (circular or elongated) (Alqahtani & Qaddah, 2019).
- Circularity ratio (R_c): Another measure of the basin's shape, based on the ratio of a circle's area to its circumference, relative to the basin perimeter, indicating whether the basin is elongated or more circular (Obeidat et al., 2021).
- Length of overland flow (l_o): Measures the length of surface flow before concentration in the stream segments, with higher values indicating greater likelihood of flooding (Horton, 1945; Sutradhar & Mondal, 2023).
- Compactness ratio (C_c): Indicates basin shape and potential flash flood susceptibility, calculated as the ratio between the basin's perimeter and a circle's perimeter with the same area (Dutal, 2023).

Lastly, the description of each parameter related to relief, summarized in Table 3:

- Basin relief (H): The difference between the highest and lowest elevations in the basin.
- Relief ratio (R_r): The ratio between basin relief and the longest stream segment, serving as an indirect measure of the main river's slope.

Table 1. Linear morphometric parameters used in the comparative analysis between the watersheds.

Morphometric parameter	Formulae (unit)	Reference
Stream order (S_u)	Strahlers' rank	Strahler (1952)
Total stream number (N_u)	$N_u = N_1 + N_2 + \ldots + N_n$	Horton (1945)
Total stream length (L_u)	$L_u = L_1 + L_2 + \ldots + L_n$ (km)	Horton (1945)
Mainstream length (L_{ms})	Geoprocessing (km)	-
Stream length ratio (R_l)	$R_l = L_u / L_{u-1}$	Horton (1945)
Mean stream length (L_{um})	$L_{um} = L_u / N_u$ (km)	Horton (1945)
Bifurcation ratio (R_b)	$R_b = N_u / N_{u+1}$	Horton (1945)
Stream length/Bifurcation ratio (ρ)	$\rho = R_l / R_b$	Horton (1945)

where L_{u-1} is the total length of the order less than L_u.

Table 2. Morphometric parameters related to the area used in the comparative analysis between the watersheds.

Morphometric parameter	Formulae (unit)	Reference
Basin area (A)	Geoprocessing (km²)	-
Basin perimeter (P)	Geoprocessing (km)	-
Drainage density (D_d)	$D_d = L_u / A$ (km/km²)	Horton (1945)
Stream frequency (F_s)	$F_s = N_u / A$ (Nu/km²)	Horton (1945)
Texture ratio (R_t)	$R_t = N_u / P$ (Nu/km)	Smith (1950)
Elongation ratio (R_e)	$R_e = (2 / L_{ms}) \times \sqrt{A / \pi}$	Schumm (1956)
Circularity ratio (R_c)	$R_c = 4 \times \pi \times A / P^2$	Schumm (1956)
Length of overland flow (l_o)	$l_o = D_d / 2$ (km²/km)	Horton (1945)
Compactness ratio (C_c)	$C_c = P / 2 \times \sqrt{\pi \times A}$	Horton (1932)

Table 3. Morphometric parameters related to relief used in the comparative analysis between the watersheds.

Morphometric parameter	Formulae (unit)	Reference
Basin relief (H)	$H = H_{max} - H_{min}$ (m)	Schumm (1956)
Relief ratio (R_r)	$R_r = H / L_{ms}$ (m/km)	Schumm (1956)
Slope (S)	Geoprocessing (rad)	-
Infiltration number (N_i)	$N_i = D_d \times F_s$	Alqahtani & Qaddah (2019)
Topographic wetness index (TWI)	$TWI = \ln\left(A / \tan(\beta)\right)$	Beven & Kirkby (1979)
Relative topographic position (RTP)	$RTP = \begin{cases} (Z_0 - \mu) / (\mu - Z_{min}), \text{if } Z_0 < \mu \\ (Z_0 - \mu) / (Z_{max} - \mu), \text{ if } Z_0 > \mu \end{cases}$	Newman et al. (2018)

where β is the slope in radians; Z_0 is the elevation of the central cell compared to the neighboring cells; and μ is the average elevation of the neighboring cells.

- Slope (S): Represents the basin's average slope. Higher values indicate greater discharge and higher flash floods susceptibility (Alqahtani & Qaddah, 2019).
- Infiltration number (N_i): Evaluates infiltration capacity indirectly, based on drainage density and stream frequency. Lower values suggest greater infiltration capacity and less surface runoff (Tola & Shetty, 2022).
- Topographic wetness index (TWI): Relates contributing area to terrain slope, quantifying topography's effect on flood generation (Tola & Shetty, 2022).
- Relative topographic position (RTP): Represents the average elevation value of a point relative to its neighbors, distinguishing valleys from watershed divides (Newman et al., 2018).

Boxplots were generated to visually identify and compare morphometric parameters between basins with differing flood exposure. To complement the visual analysis, the non-parametric Mann-Whitney test (Mann & Whitney, 1947), also known as the U-test, was applied to assess whether observed differences between independent samples were statistically significant (at a significance level of 0.05) or attributable to random variation.

Floodplain topography

To assess whether differences exist between the topographies of floodplains in regions more exposed to flooding compared to less exposed areas, an elevation profile analysis was conducted using a graph of flooded elevation versus flooded area.

To generate the graph, the outlets of the basins, corresponding to the locations of the gauge stations, were first defined (Figure 2a). For each outlet, a cross-section was then drawn, extending to the water divide (Figure 2b). The extent of these cross-sections was determined using Height Above the Nearest Drainage (HAND) (Nobre et al., 2011), aiming to represent the valley geometry. Based on this cross-section, a circle was delineated using three points: the two end points of the the cross-section (defining the secant of the circle) and a third point located at a distance twice the length of the secant, following the meanders of the main drainage network (Figure 2c). This circle was considered the approximated area of the floodplain (Figure 2d).

The initial methodology intended to use the floodplain data from the GFPLAIN250m floodplain database (Nardi & Annis, 2018). However, due to its low spatial resolution, some locations lacked floodplain representation, necessitating an adapted methodology. Thus, the operations described above and illustrated in Figure 2, while simplified, aims to capture approximate floodplains area. This novel methodology, developed specifically for this study, addresses the limitations of the GFPLAIN250m dataset and, to the authors' knowledge, has not been documented in prior research.

Flood elevation heights and flooded areas were determined using the DEM and the terrain descriptor model HAND. For each of the 56 floodplain representations, the elevation profile was extracted based on HAND values, and the corresponding flooded area was calculated to generate a graph of elevation (HAND values limited to 30 meters) versus flooded area (expressed as a percentage).

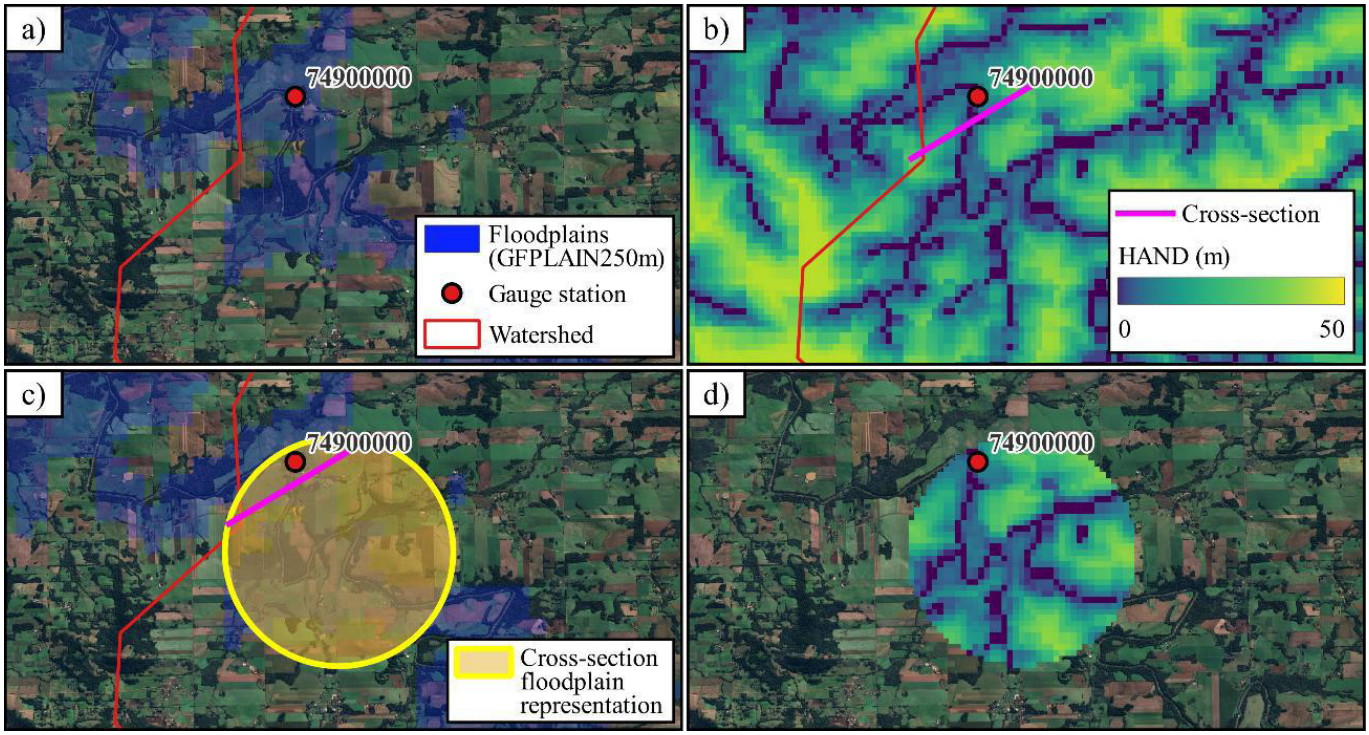

Figure 2. Illustration of the procedure used to obtain data for the flood elevation versus flooded area graph, where: (a) represents the outlet; (b) represents the cross-section; (c) represents the floodplain approximated as a circle; (d) shows the data for the Flood Elevation versus Flooded Area graph. Source: DEM SRTM (Farr et al., 2007), CAMELS-BR gauge stations (Chagas et al., 2020), GFPLAIN250m Floodplain (Nardi & Annis, 2018).

An exponential equation of the form $y = a \cdot x^b$ was fitted to each graph, and the *b* values were analyzed to compare results between gauge stations in areas more exposed to flooding and those in less exposed areas. While other models might also be suitable, and a more rigorous analysis comparing other model fits could be performed in future work, the exponential function was chosen because its general form appeared to capture the observed non-linear relationship between elevation and flooded area in most cases. This model also allowed for a relatively simple comparison of the parameter *b* between gauge stations.

In addition to the topographic analysis, flood frequency curves were compared for each gauge station, using the same categorization: areas more exposed to flooding versus less exposed areas. A hydrological frequency analysis was conducted to determine return periods associated with annual maximum discharge, which were then used to evaluate the flood frequency.

RESULTS AND DISCUSSION

Morphometric relationships

The morphometric differences between the watersheds were evaluated by comparing parameter values using boxplot charts. This approach facilitates understanding the disparities, especially when comparing watersheds more exposed to flooding with those less exposed. Figure 3 presents the set of selected morphometric parameters (as detailed in Tables 1 to 3), differentiating the watershed categories (more or less flood exposed) and highlighting the U-test results, which assessed the statistical differences between the data.

Analyzing the results of the linear parameters (Table 1), it was observed that Stream order (S_u), Total stream number (N_u), and Total stream length (L_u) showed statistically significant differences between watersheds more or less exposed to flooding.

Watersheds with higher S_u, N_u, and L_u values were more prone to flooding, consistent with the literature for these parameters: higher S_u values are associated with greater flow and surface runoff velocity (Obeidat et al., 2021; Romshoo et al., 2012), and higher N_u values indicate greater elevation differences in the basin, steeper slopes, and consequently higher susceptibility to flooding, particularly flash floods (Tola & Shetty, 2022). For the remaining linear parameters — Mainstream length (L_{ms}), Stream length ratio (R_l), Mean stream length (L_{um}), Bifurcation ratio (R_b), and Stream length/Bifurcation ratio (ρ) — no statistically significant differences were observed between the watershed categories.

Regarding area-related parameters (Table 2), the results indicated that Basin area (*A*), Basin perimeter (P), Texture ratio (R_t), Circularity ratio (R_c), and Compactness ratio (C_c) exhibited statistically significant differences between watersheds more or less exposed to flooding. Watersheds with higher *A*, *P*, R_p, and C_c values tended to be more flood-prone. This is partially explained in recent literature, as *A* is significant in determining the volume of water that can generate surface runoff from precipitation (Obeidat et al., 2021).

The parameters R_c and C_c relate to the comparison of basin area and perimeter with a circular basin's characteristics. R_c represents the ratio of the basin area to the area of a circle with the same perimeter, while C_c is the ratio of the basin perimeter to the perimeter of a circle with the same area. Both parameters illustrate basin characteristics influencing flood response: higher R_c and C_c values closer to 1 indicate a more circular basin, which, due to shorter response times, is more susceptible to flooding, particularly flash floods (Abdo, 2020; Bhat et al., 2019; Dutal, 2023; Tola & Shetty, 2022).

The R_t parameter is an indicator of basin texture. Higher values indicate a finer texture with more river segments, suggesting reduced infiltration and increased flood susceptibility (Tola & Shetty, 2022), consistent with the results obtained. On the other hand, *P*, an indicator of basin size and shape (Rana & Suryanarayana, 2021), was less frequently discussed in the studied literature. Finally, Drainage density (D_d), Stream frequency (F_s), Elongation ratio (R_e), and Length of overland flow (I_o) did not show statistically significant differences.

For the relief-related parameters (Table 3), only the Relative Topographic Position (*RTP*) showed statistically significant differences. The *RTP* function represents the elevation difference of a DEM cell compared to its neighbors, relative to the maximum, minimum, and average elevation of the neighboring cells (Newman et al., 2018). Its results can be interpreted as follows: positive values indicate crest cells, and negative values indicate valley cells. This aligns with the observed results, as lower *RTP* values were associated with more flood-prone watersheds. The other parameters — Basin Relief (*H*), Relief ratio (R_r), Slope (*S*), Infiltration number (N_i), and Topographic wetness index (*TWI*) — did not show differences between the watershed categories.

According to the methodology used in this study, the primary morphometric parameters influencing flooding in the RS are those related to basin shape, categorized here as linear (S_u, N_u, and L_u) and area-related (*A*, *P*, R_p, R_c, and C_c). Among the relief-related parameters, only *RTP* showed statistical differences when comparing the watersheds. These results suggest that in the study region, gauge stations located in larger watersheds with longer rivers and denser and more extensive drainage networks are more prone to flooding. Similarly, stations located in watersheds with larger areas, perimeters, and more elongated shapes were more flood-prone, indicating that the shapes of flood-prone basins are more associated with long-term flooding compared to others.

Floodplain topography

In the analysis of floodplain topography, based on the streamflow monitoring gauge stations used in this study, cross-sections were drawn at the outlets of each watershed, and the floodplain area was subsequently estimated from these sections, as described in Methodology. A total of 56 floodplains were estimated.

Flood elevation versus flooded area graphs were created to investigate possible differences in floodplain shapes, particularly when comparing watersheds more or less exposed to flooding. The results for each watershed were consolidated into a single image, presented in Figure 4, which shows the mean curve for each watershed type, accompanied by a 95% confidence interval for elevation values. Additionally, the value of *b* from the exponential fitting equation ($y = a \cdot x^b$) for the mean curve is included.

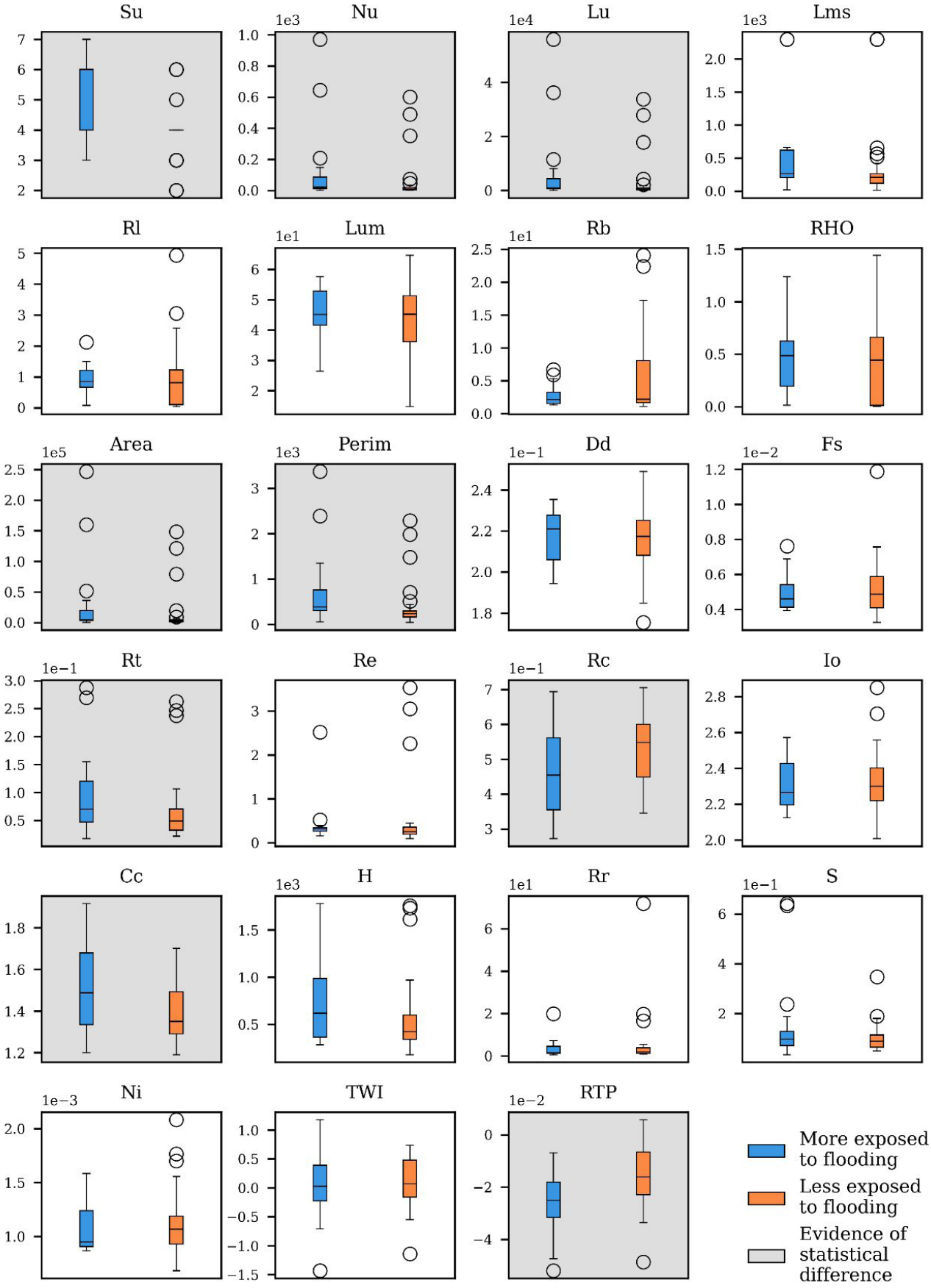

Figure 3. Comparison of the morphometric parameters of the studied watersheds, distinguishing those identified as more or less exposed to flooding.

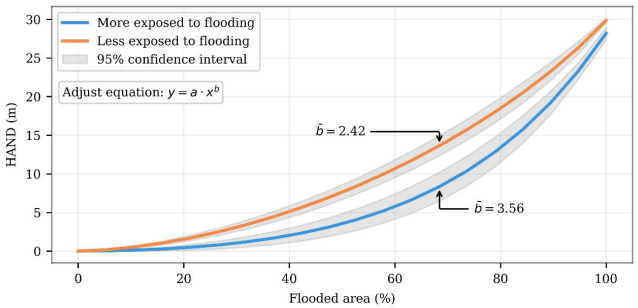

Figure 4. Mean flood elevation versus flooded area curves (limited to 30 meters of HAND) with a 95% confidence interval, grouped by gauge stations identified as more or less exposed to flooding.

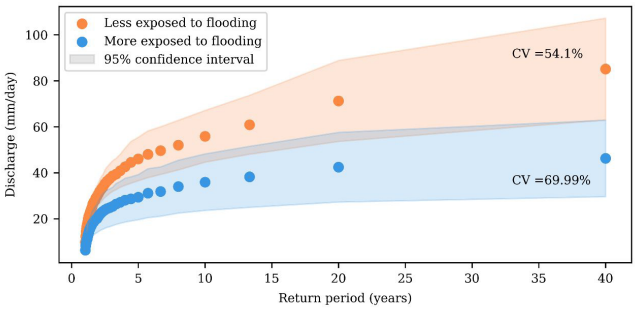

Figure 5. Mean flood frequency curves with a 95% confidence interval, grouped by gauge stations identified as more or less exposed to flooding.

The curves reveal a larger flooded area as elevation increases for watersheds more exposed to flooding ($\bar{b} = 3.56$) compared to those less exposed ($\bar{b} = 2.42$). This can be observed in the two curves and their confidence intervals, as well as in the *b* exponent value. Higher *b* values indicate a greater increase in the flooded area relative to elevation, while lower *b* values represent a smaller increase in flooded area for the same elevation increment. Values of *b* closer to 1 indicate a floodplain profile resembling the letter "V" whereas values greater than 1 suggest a profile more similar to the letter "U" The results indicate that watersheds more exposed to flooding tend to have a "U"-shaped profile, whereas less exposed watersheds exhibit a "V"-shaped profile.

According to Das (2019), regions located in low-altitude floodplains are more exposed to flooding compared to mountainous areas. This observation aligns with Figure 4, where floodplain regions—with larger flooded areas relative to elevation increments — are more exposed to flooding, as indicated by a higher b value. Conversely, regions less exposed to flooding exhibit smaller flooded areas for the same elevation increment.

Using a similar methodology, Devitt et al. (2023) employed the *b* term of the equation to assess floodplain sensitivity to return periods (RP). They found that *b* values greater than 1 indicate basins sensitive to higher RP values, whereas values below 1 represent basins more sensitive to shorter RP values. Additionally, they analyzed floodplain confinement types: confined, partially confined, and laterally unconstrained. Their results indicated that most river stretches analyzed had partially confined floodplains sensitive to short return periods (Devitt et al., 2023).

Figure 5 presents the results of the flood frequency curves, condensed into two curves: one for gauge stations in areas more exposed to flooding (17 gauges) and another for less exposed areas (38 gauges). These curves represent the average specific discharge for the stations, in units of mm/day, aiming to normalize discharge values proportionally to the drainage area upstream of the gauge stations. In addition to Figure 5, flood frequency curves for instantaneous discharge values in m^3/s and individual gauge station curves are provided in Appendix A.

The results of the mean flood frequency curves indicate that the average specific discharge is lower for watersheds more exposed to flooding than for less exposed watersheds across all return period intervals. Contrary to the initial expectation that basins more exposed to flooding would exhibit higher discharge values, morphometric analysis revealed that these basins tend to have significantly larger drainage areas, and the presence of more extensive floodplains may have played a crucial role in this unexpected behavior. This observation is reinforced by a recent study by Paiva & Lima (2024), which identified floodplains as one key factor in attenuating flood waves, thus explaining the results obtained.

In a similar approach, Devitt et al. (2023) used the *b* term of the equation to evaluate floodplain sensitivity to RP and confinement of river stretches, finding that basins sensitive to shorter RP values were predominantly partially confined, whereas basins sensitive to longer RP values were mostly confined. Comparing these results with the findings of this study, watersheds more exposed to flooding appear to align with partially confined floodplains (Figure 4), suggesting more elongated floodplain shapes.

This study, while achieving its objectives, raises a few limitations and questions that can be investigated in future work to improve the methodology and broaden its applicability. First, a limitation observed in this study lies in the choice of the DEM. A sensitivity analysis of the results using other types of DEMs with enhanced spatial resolution (30 meters or less) was not performed and could improve the results.

Another point is that, to compare basins and their topography, both in relation to morphometric parameters and the shape of the floodplain profile, they need to be pre-classified according to their flood susceptibility. This classification can be done based on historical records, such as those used in this work, or, in the absence of such data, through the analysis of the morphometric parameters themselves, as proposed by Obeidat et al. (2021), for example.

Finally, future research could integrate information such as land use and cover, climate conditions, and demographics with morphometric characteristics. The application of machine learning techniques could be particularly valuable in identifying correlations between these diverse attributes. These studies could contribute to a more comprehensive understanding of flood dynamics and enhance the applicability of this methodology for watershed management and flood risk mitigation.

CONCLUSION

This study investigated the influence of topography on flooding in southern Brazil from two perspectives: morphometric

parameters and floodplains. Watersheds in the region were categorized as either more exposed or less exposed to flooding, and the results of this analysis were compared.

The analyzed morphometric parameters revealed significant differences between watersheds more and less exposed to flooding, particularly in parameters directly or indirectly related to basin size. Larger watersheds, characterized by greater area, perimeter, and drainage network extent, were found to be the most flood-prone. Regarding relief, only the indirect parameter, RTP showed significant differences.

In terms of floodplain topography, watersheds with higher flood exposure exhibited profiles resembling a "U" shape, while those less exposed to flooding displayed profiles closer to a "V" shape. This indicates that, for the same elevation level measured using the HAND, the floodable area of more exposed watersheds was larger than that of less exposed watersheds, underscoring the topographic distinctions between the two categories.

The analysis of the flood frequency revealed higher specific discharge values for watersheds less exposed to flooding compared to the more exposed, for the same return period. This suggests that the "U"-shaped floodplain valleys in the more exposed watersheds may play a role in attenuating discharge during flood events. Furthermore, this observation could indicate that the basins most exposed to flooding are more affected by fluvial floods than flash floods. Further investigations are recommended to validate this assumption.

The proposed methodology successfully identified measurable morphometric parameters derived from DEM that can distinguish regions through a simplified analysis. Combined with the comparison of floodplain relief profiles, these methods could serve as a preliminary tool to assist public authorities in watershed management and flood risk mitigation. However, it is significant to acknowledge the limitations of this study and consider its applicability in other contexts.

It is important to note that potential changes in flood regimes due to climate change were not considered in this study. From the perspective of morphometric parameters, the impact of climate change is expected to be minimized; however, further analysis incorporating this perspective is recommended.

ACKNOWLEDGEMENTS

I would like to thank my colleagues from the Hidrologia de Grande Escala (HGE) research group for their support and the professors of the Institute of Hydraulic Research (IPH) at Universidade Federal do Rio Grande do Sul (UFRGS) for the quality public education.

REFERENCES

Abdo, H. G. (2020). Evolving a total-evaluation map of flash flood hazard for hydro-prioritization based on geohydromorphometric parameters and GIS–RS manner in Al-Hussain river basin, Tartous, Syria. *Natural Hazards*, *104*(1), 681-703. http://doi.org/10.1007/s11069-020-04186-3.

Alqahtani, F., & Qaddah, A. A. (2019). GIS digital mapping of flood hazard in Jeddah–Makkah region from morphometric analysis. *Arabian Journal of Geosciences*, *12*(6), 199. http://doi.org/10.1007/s12517-019-4338-8.

Ávila, B. T., Almeida Neto, J. O. D., & Felippe, M. F. (2017). Suscetibilidade morfométrica a inundações nas bacias hidrográficas tributárias do Rio do Peixe, zona da mata de Minas Gerais. *Formação*, *1*(24), http://doi.org/10.33081/formacao.v1i24.4905.

Basahi, J., Masoud, M., & Zaidi, S. (2016). Integration between morphometric parameters, hydrologic model, and geo-informatics techniques for estimating WADI runoff (case study WADI HALYAH: saudi Arabia). *Arabian Journal of Geosciences*, *9*(13), 610. http://doi.org/10.1007/s12517-016-2649-6.

Berte, A. M. A., Lemos, B. O., Mieres, L. S., Oliveira, S. B., Paranhos, A. J. V., & Silva, C. R. (2022). *Desastres naturais no Rio Grande do Sul: estudo sobre as ocorrências no período 2003-2021*. Porto Alegre: Secretaria de Planejamento, Governança e Gestão.

Beven, K. J., & Kirkby, M. J. (1979). A physically based, variable contributing area model of basin hydrology / Un modèle à base physique de zone d'appel variable de l'hydrologie du bassin versant. *Hydrological Sciences Bulletin*, *24*(1), 43-69. http://doi.org/10.1080/02626667909491834.

Bhat, M. S., Alam, A., Ahmad, S., Farooq, H., & Ahmad, B. (2019). Flood hazard assessment of upper Jhelum basin using morphometric parameters. *Environmental Earth Sciences*, *78*(2), 54. http://doi.org/10.1007/s12665-019-8046-1.

Blöschl, G. (2022). Three hypotheses on changing river flood hazards. *Hydrology and Earth System Sciences*, *26*(19), 5015-5033. http://doi.org/10.5194/hess-26-5015-2022.

Brêda, J. P. L. F., Cauduro Dias De Paiva, R., Siqueira, V. A., & Collischonn, W. (2023). Assessing climate change impact on flood discharge in South America and the influence of its main drivers. *Journal of Hydrology (Amsterdam)*, *619*, 129284. http://doi.org/10.1016/j.jhydrol.2023.129284.

Chagas, V. B. P., Chaffe, P. L. B., Addor, N., Fan, F. M., Fleischmann, A. S., Paiva, R. C. D., & Siqueira, V. A. (2020). CAMELS-BR: hydrometeorological time series and landscape attributes for 897 catchments in Brazil. *Earth System Science Data*, *12*(3), 2075-2096. http://doi.org/10.5194/essd-12-2075-2020.

Chagas, V. B. P., Chaffe, P. L. B., & Blöschl, G. (2022). Process controls on flood seasonality in Brazil. *Geophysical Research Letters*, *49*(5), e2021GL096754.

Chaithong, T. (2022). Flash flood susceptibility assessment based on morphometric aspects and hydrological approaches in the Pai River Basin, Mae Hong Son, Thailand. *Water*, *14*(19), 3174. http://doi.org/10.3390/w14193174.

Collischonn, W., Brêda, J. P. F., Wongchuig, S., Ruhoff, A., Paiva, R. C. D., Fan, F. M., Filho, R. C., & Ramalho, N. (2024). Unprecedented April-May 2024 rainfall in South Brazil sets new record. *Revista Brasileira de Recursos Hídricos*, *29*(50), 16.

Das, S. (2019). Geospatial mapping of flood susceptibility and hydro-geomorphic response to the floods in Ulhas basin, India. *Remote Sensing Applications: Society and Environment*, *14*, 60-74. http://doi.org/10.1016/j.rsase.2019.02.006.

Devitt, L., Neal, J., Coxon, G., Savage, J., & Wagener, T. (2023). Flood hazard potential reveals global floodplain settlement patterns. *Nature Communications*, *14*(1), 2801. http://doi.org/10.1038/s41467-023-38297-9.

Dutal, H. (2023). Using morphometric analysis for assessment of flash flood susceptibility in the Mediterranean region of Turkey. *Environmental Monitoring and Assessment*, *195*(5), 582. http://doi.org/10.1007/s10661-023-11201-0.

Farr, T. G., Rosen, P. A., Caro, E., Crippen, R., Duren, R., Hensley, S., Kobrick, M., Paller, M., Rodriguez, E., Roth, L., Seal, D., Shaffer, S., Shimada, J., Umland, J., Werner, M., Oskin, M., Burbank, D., & Alsdorf, D. (2007). The shuttle radar topography mission. *Reviews of Geophysics*, *45*(2), 2005RG000183. http://doi.org/10.1029/2005RG000183.

Franco, A. C. V., & Santo, M. A. D. (2015). Contribution of morphometry to flood studies in the Luís Alves basin/SC, Brazil. *Mercator*, *14*(3), 151-167. http://doi.org/10.4215/RM2015.1403.0009.

G1 (2024, 2 de julho). Sobe para 182 número de vítimas após enchente no RS; 29 pessoas seguem desaparecidas. *G1*. Retrieved in 2025, January 14, from https://g1.globo.com/rs/rio-grande-do-sul/noticia/2024/07/02/enchentes-no-rs-total-de-mortos-e-desaparecidos.ghtml>

Gnann, S., Baldwin, J. W., Cuthbert, M. O., Gleeson, T., Schwanghart, W., & Wagener, T. (2025). The influence of topography on the global terrestrial water cycle. *Reviews of Geophysics*, *63*(1), e2023RG000810. http://doi.org/10.1029/2023RG000810.

Horton, R. E. (1932). Drainage-basin characteristics. *Transactions - American Geophysical Union*, *13*(1), 350-361. http://doi.org/10.1029/TR013i001p00350.

Horton, R. E. (1945). Erosional development of streams and their drainage basins: hydrophysical approach to quantitative morphology. *Geological Society of America Bulletin*, *56*(3), 275. http://doi.org/10.1130/0016-7606(1945)56[275:EDOSAT]2.0.CO;2.

Koralay, N., & Kara, Ö. (2023). Effects of morphometric characteristics on flood in Degirmendere sub-watersheds, Northeastern Turkey. *International Journal of River Basin Management*, *21*(2), 327-337. http://doi.org/10.1080/15715124.2021.1981355.

Mahmoodi, E., Azari, M., & Dastorani, M. T. (2023). Comparison of different objective weighting methods in a multi-criteria model for watershed prioritization for flood risk assessment using morphometric analysis. *Journal of Flood Risk Management*, *16*(2), e12894. http://doi.org/10.1111/jfr3.12894.

Mann, H. B., & Whitney, D. R. (1947). On a test of whether one of two random variables is stochastically larger than the other. *Annals of Mathematical Statistics*, *18*(1), 50-60. http://doi.org/10.1214/aoms/1177730491.

Marcuzzo, F. F. N., Kenup, R. E., Zanetti, H. P., Oliveira, M. P., Wilson, E. da S., Acosta, C. C., & Bao, R. (2024). *Nota técnica: aferição direta e avaliação indireta do nível máximo de rios do rio grande do sul na grande cheia de maio de 2024* (5ª versão). Retrieved in 2025, January 14, from https://rigeo.sgb.gov.br/handle/doc/24939.7

Menezes, D. J., & Sccoti, A. A. V. (2013). Inventário de Registro de Inundações no Estado do Rio Grande do Sul entre 1980 e 2010. In L. E. S. Robaina, & R. Trentin (Eds.), *Desastres naturais do Rio Grande do Sul*. Santa Maria: Editora UFSM.

Merz, B., Blöschl, G., Vorogushyn, S., Dottori, F., Aerts, J. C. J. H., Bates, P., Bertola, M., Kemter, M., Kreibich, H., Lall, U., & MacDonald, E. (2021). Causes, impacts and patterns of disastrous river floods. *Nature Reviews Earth & Environment*, *2*(9), 592-609. http://doi.org/10.1038/s43017-021-00195-3.

Nardi, F., & Annis, A. (2018). *GFPLAIN250m*. Figshare. http://doi.org/10.6084/M9.FIGSHARE.6665165.V1.

Nasir, M. J., Iqbal, J., & Ahmad, W. (2020). Flash flood risk modeling of swat river sub-watershed: a comparative analysis of morphometric ranking approach and El-Shamy approach. *Arabian Journal of Geosciences*, *13*(20), 1082. http://doi.org/10.1007/s12517-020-06064-5.

Negri, R., & Fill, H. (2023). Caracterização física de 14 bacias hidrográficas brasileiras: proposição do indicador da declividade média dos rios e do coeficiente de suscetibilidade de enchentes. *Engenharia Sanitaria e Ambiental*, *28*, e20220194. http://doi.org/10.1590/s1413-415220220194.

Newman, D. R., Lindsay, J. B., & Cockburn, J. M. H. (2018). Evaluating metrics of local topographic position for multiscale geomorphometric analysis. *Geomorphology*, *312*, 40-50. http://doi.org/10.1016/j.geomorph.2018.04.003.

Nobre, A. D., Cuartas, L. A., Hodnett, M., Rennó, C. D., Rodrigues, G., Silveira, A., Waterloo, M., & Saleska, S. (2011). Height Above the Nearest Drainage – a hydrologically relevant new terrain model. *Journal of Hydrology (Amsterdam)*, *404*(1–2), 13-29. http://doi.org/10.1016/j.jhydrol.2011.03.051.

Obeidat, M., Awawdeh, M., & Al-Hantouli, F. (2021). Morphometric analysis and prioritisation of watersheds for flood risk management in Wadi Easal Basin, Jordan, using geospatial technologies. *Journal*

of Flood Risk Management, *14*(2), e12711. http://doi.org/10.1111/jfr3.12711.

Paiva, R. C. D., & Lima, S. G. (2024). A simple model of flood peak attenuation. *Water Resources Research*, *60*(2), e2023WR034692. http://doi.org/10.1029/2023WR034692.

Rana, V. K., & Suryanarayana, T. M. V. (2021). Estimation of flood influencing characteristics of watershed and their impact on flooding in data-scarce region. *Annals of GIS*, *27*(4), 397-418. http://doi.org/10.1080/19475683.2021.1960603.

Reboita, M. S., Mattos, E. V., Capucin, B. C., Souza, D. O. D., & Ferreira, G. W. D. S. (2024). A multi-scale analysis of the extreme precipitation in southern Brazil in april/may 2024. *Atmosphere*, *15*(9), 1123. http://doi.org/10.3390/atmos15091123.

Rio Grande do Sul. (2024). *Mapa Único Plano Rio Grande*. Retrieved in 2025, January 14, from https://mup.rs.gov.br/

Romshoo, S. A., Bhat, S. A., & Rashid, I. (2012). Geoinformatics for assessing the morphometric control on hydrological response at watershed scale in the Upper Indus Basin. *Journal of Earth System Science*, *121*(3), 659-686. http://doi.org/10.1007/s12040-012-0192-8.

Schumm, S. A. (1956). Evolution of drainage systems and slopes in badlands at Perth Amboy, New Jersey. *Geological Society of America Bulletin*, *67*(5), 597. http://doi.org/10.1130/0016-7606(1956)67[597:EODSAS]2.0.CO;2.

Smith, K. G. (1950). Standards for grading texture of erosional topography. *American Journal of Science*, *248*(9), 655-668. http://doi.org/10.2475/ajs.248.9.655.

Strahler, A. N. (1952). Hypsometric (area-altitude) analysis of erosional topography. *Geological Society of America Bulletin*, *63*(11), 1117. http://doi.org/10.1130/0016-7606(1952)63[1117:HAAOET]2.0.CO;2.

Sutradhar, S., & Mondal, P. (2023). Prioritization of watersheds based on morphometric assessment in relation to flood management: a case study of Ajay river basin, Eastern India. *Watershed Ecology and the Environment*, *5*, 1-11. http://doi.org/10.1016/j.wsee.2022.11.011.

Tola, S. Y., & Shetty, A. (2022). Flood susceptibility modeling based on morphometric parameters in Upper Awash River basin, Ethiopia using geospatial techniques. *Sustainable Water Resources Management*, *8*(2), 49. http://doi.org/10.1007/s40899-022-00642-z.

Vale, J. R. B., & Bordalo, C. A. L. (2020). CAracterização morfométrica e do uso e cobertura da terra da bacia hidrográfica do rio Apeú, Amazônia Oriental. *Formação*, *27*(51), http://doi.org/10.33081/formacao.v27i51.6026.

van Appledorn, M., Baker, M. E., & Miller, A. J. (2019). River-valley morphology, basin size, and flow-event magnitude interact to produce wide variation in flooding dynamics. *Ecosphere*, *10*(1), e02546. http://doi.org/10.1002/ecs2.2546.

Authors contributions

Vinícius Kuchinski: Conceptualization, data curation, methodology, investigation, writing – original draft.

Rodrigo Cauduro Dias de Paiva: Validation, formal analysis, resources, writing – review & editing, supervision.

Editor-in-Chief: Adilson Pinheiro

Associated Editor: Michael Männich

APPENDIX A. COMPLEMENTARY FIGURES AND DATA.

The following Figure A1 to Figure A7 present the condensed mean flood frequency curves (Figure A1) as well as the curves for each of the studied watersheds (Figure A2 to Figure A8). Unlike what is shown in the middle of the paper, these graphs display discharge in the unit m^3/s.

In these images, a vertical dashed line is included at the point where the return period (RP) equals 5 years. This line serves as a reference, as it allows for the identification of the inflection point in the curve for most stations. At this point, there is a shift in behavior, with a sharp reduction in the increase of discharge as a function of the RP.

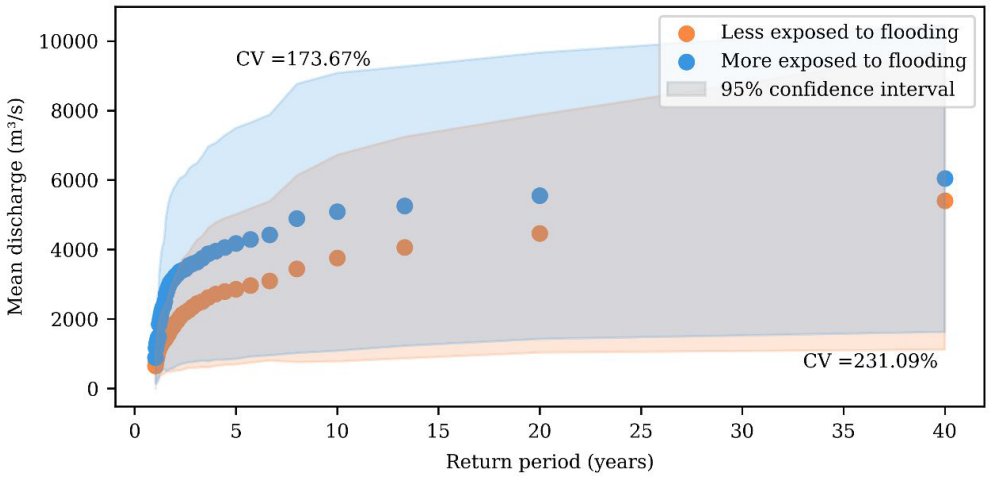

Figure A1. Mean flood frequency curves with a 95% confidence interval, grouped by gauge stations identified as more or less exposed to flooding.

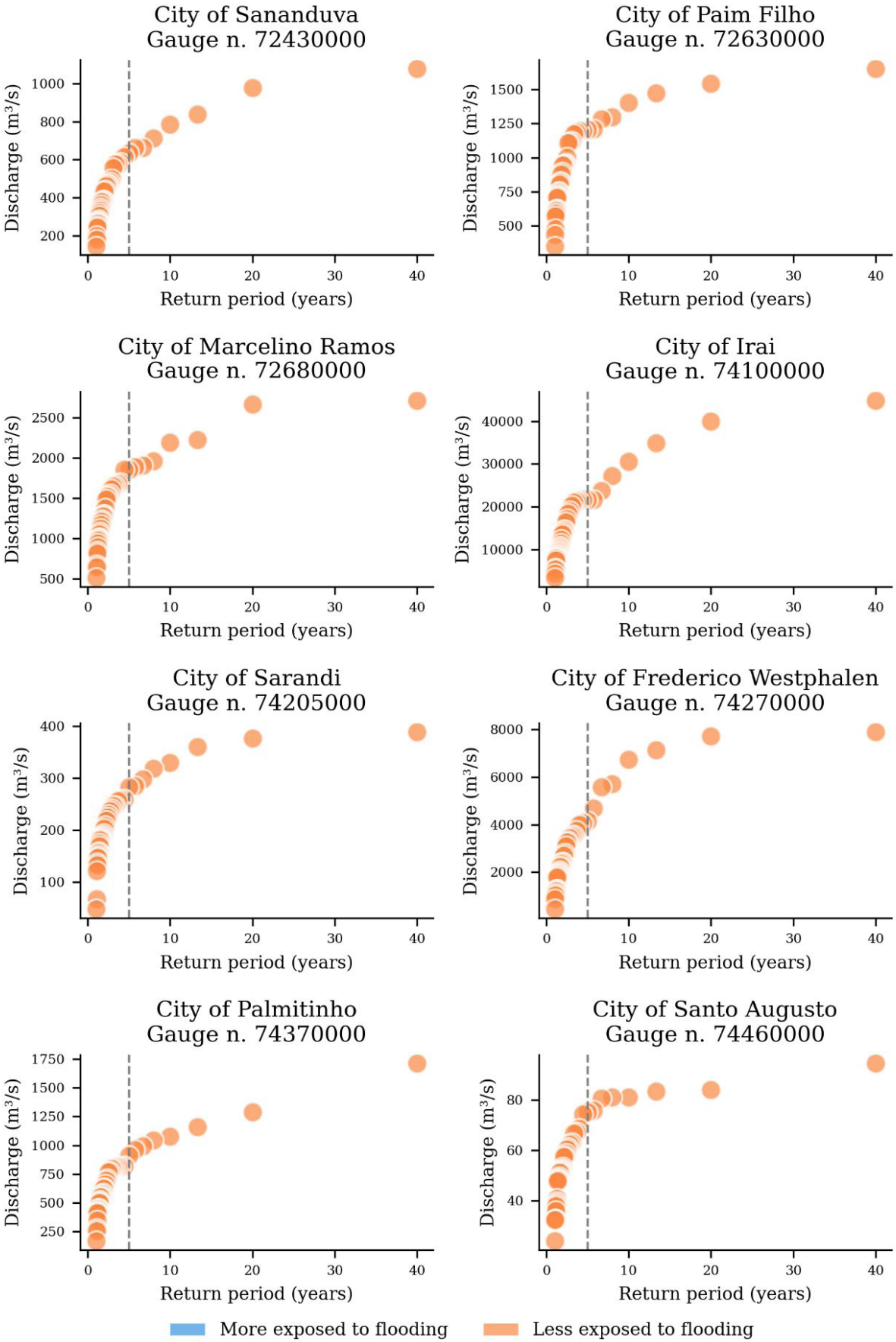

Figure A2. Flood frequency curves for the studied gauge stations, with the dashed line representing RP = 5 years, image 1 of 7.

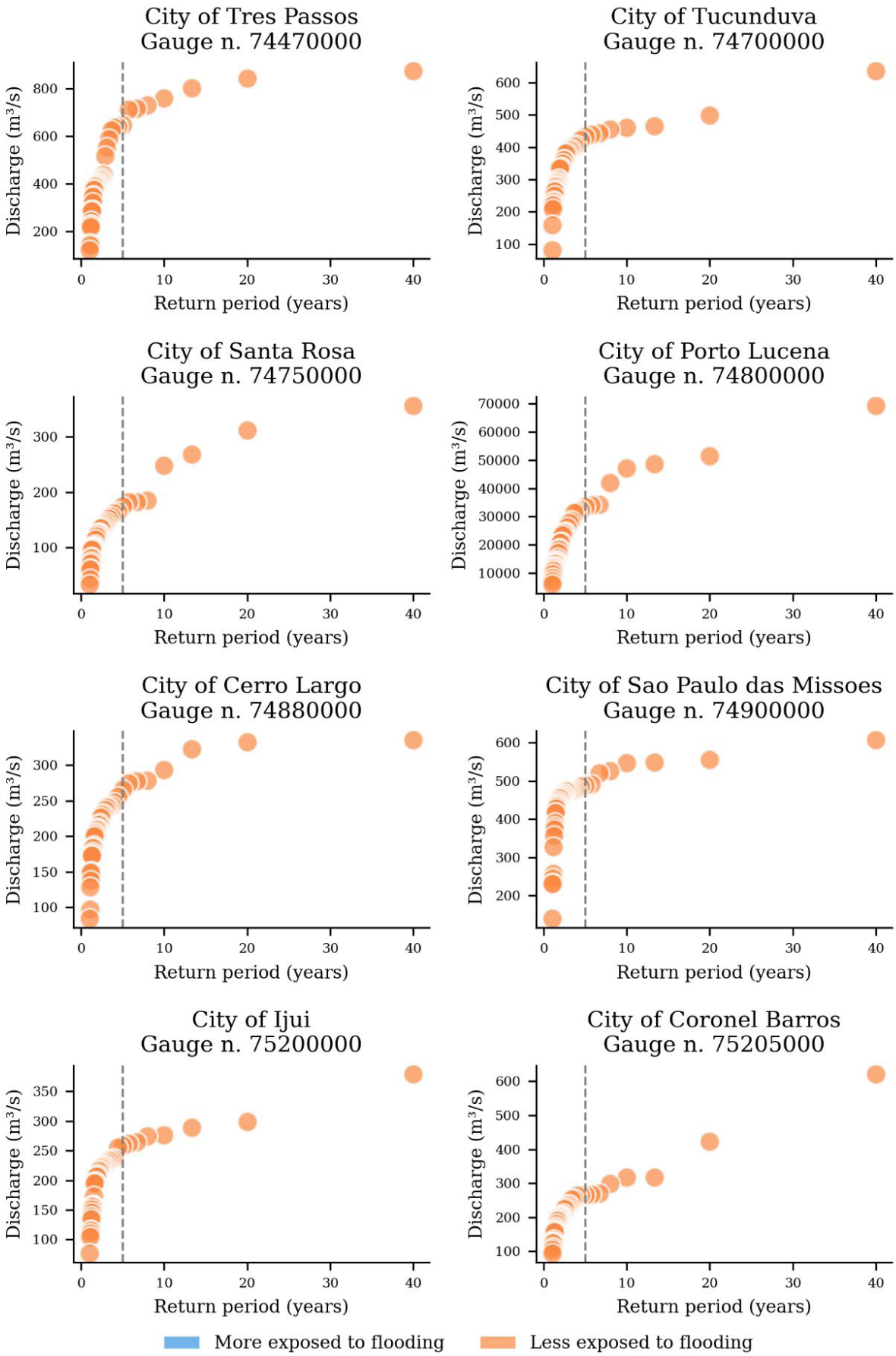

Figure A3. Flood frequency curves for the studied gauge stations, with the dashed line representing RP = 5 years, image 2 of 7.

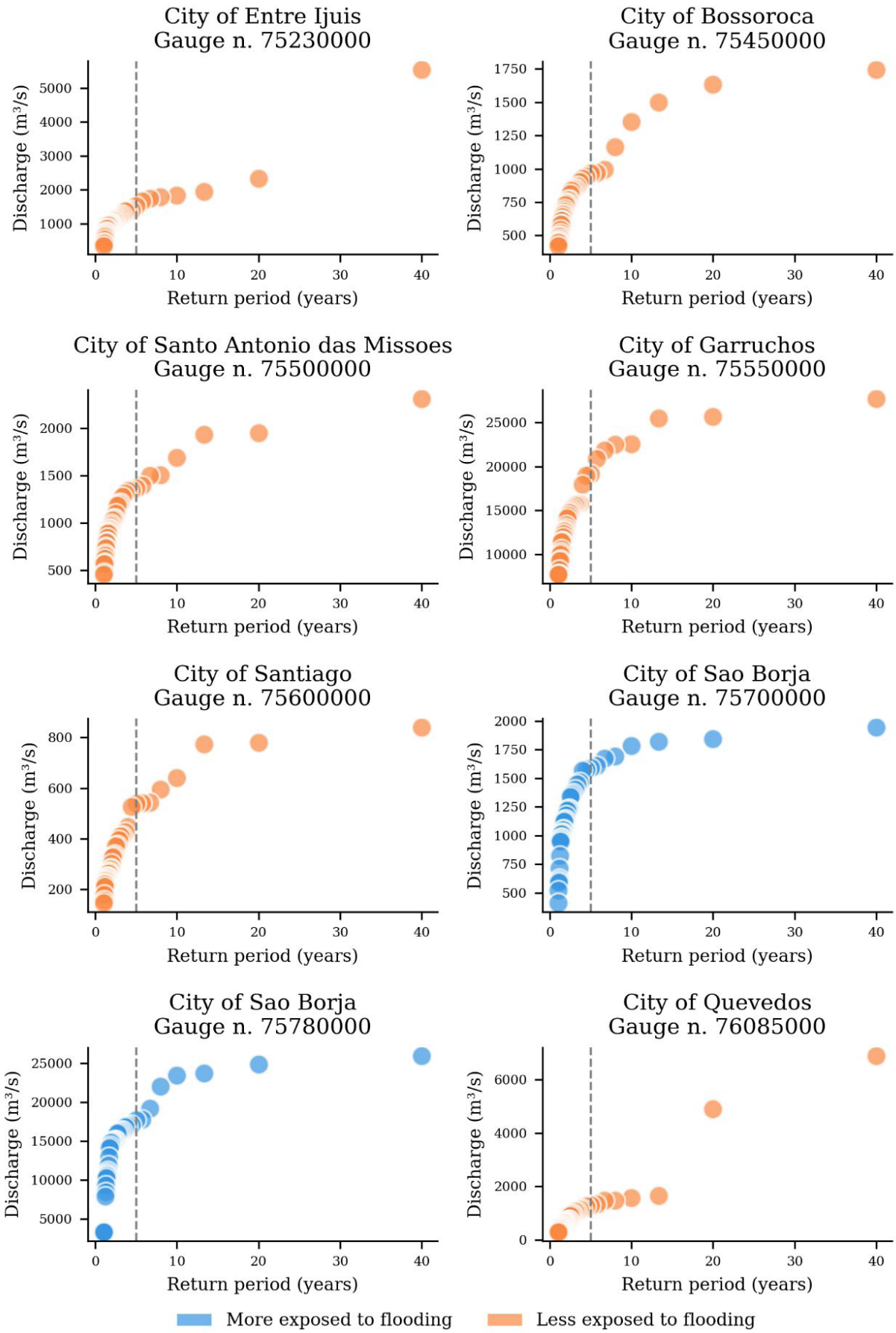

Figure A4. Flood frequency curves for the studied gauge stations, with the dashed line representing RP = 5 years, image 3 of 7.

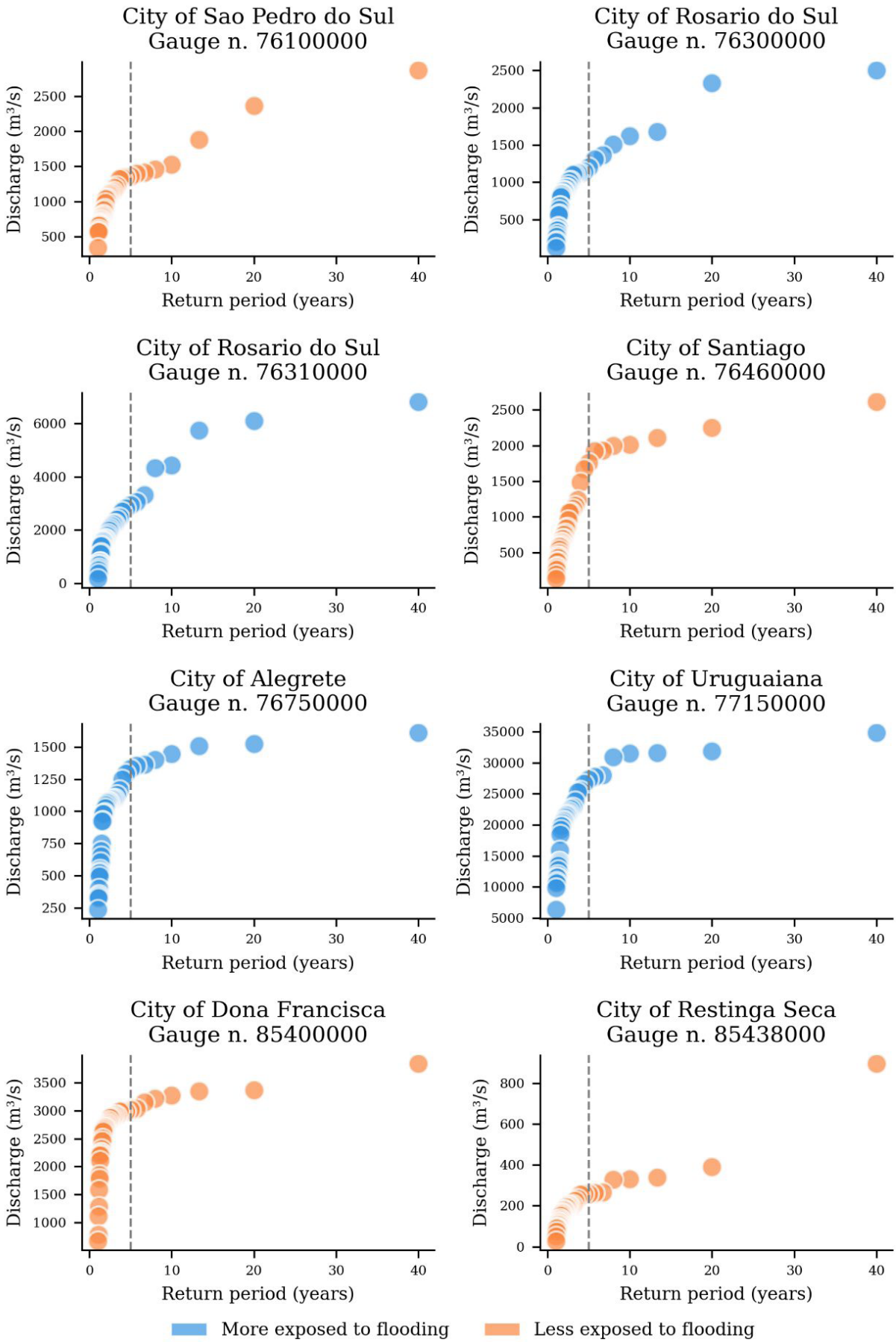

Figure A5. Flood frequency curves for the studied gauge stations, with the dashed line representing RP = 5 years, image 4 of 7

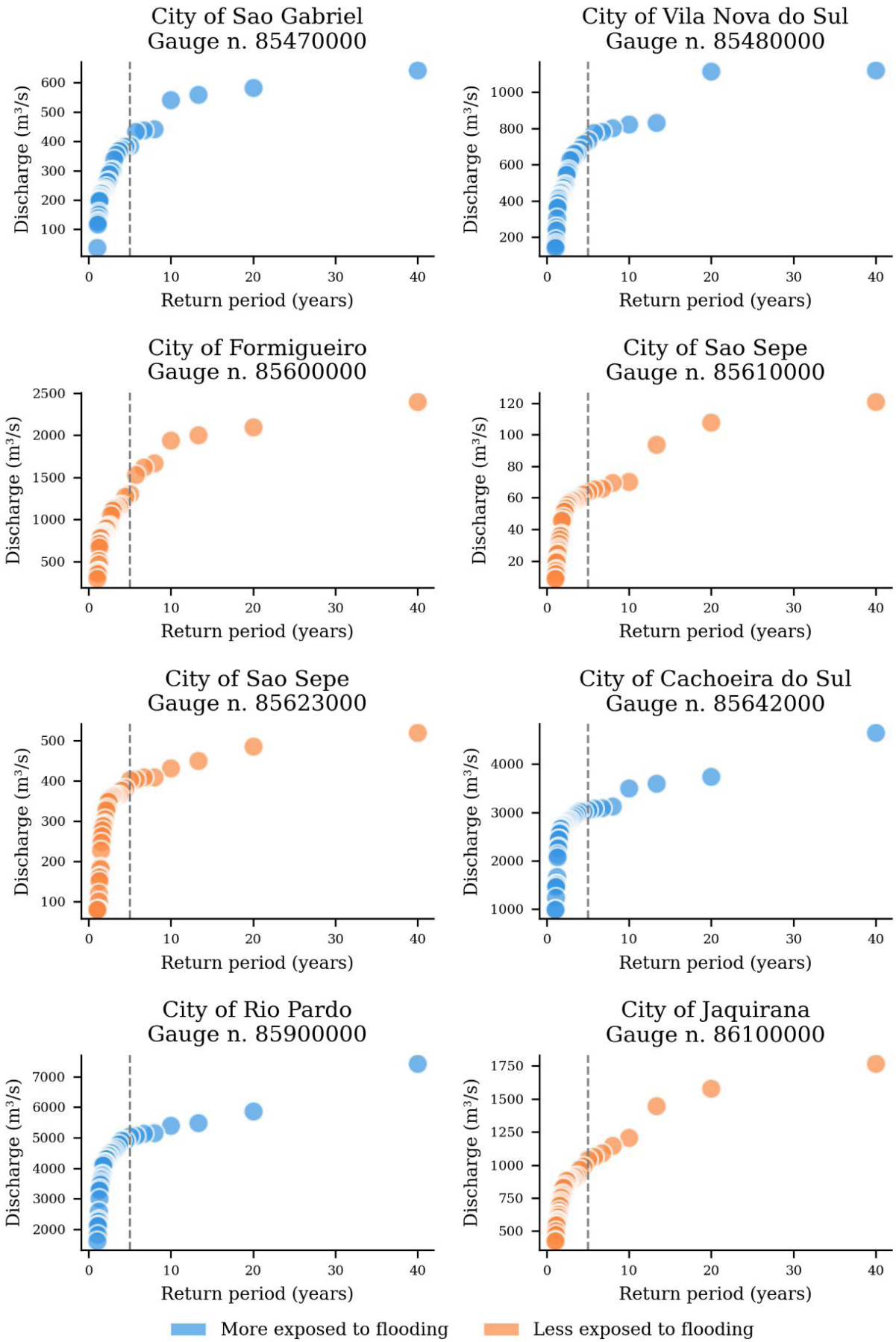

Figure A6. Flood frequency curves for the studied gauge stations, with the dashed line representing RP = 5 years, image 5 of 7.

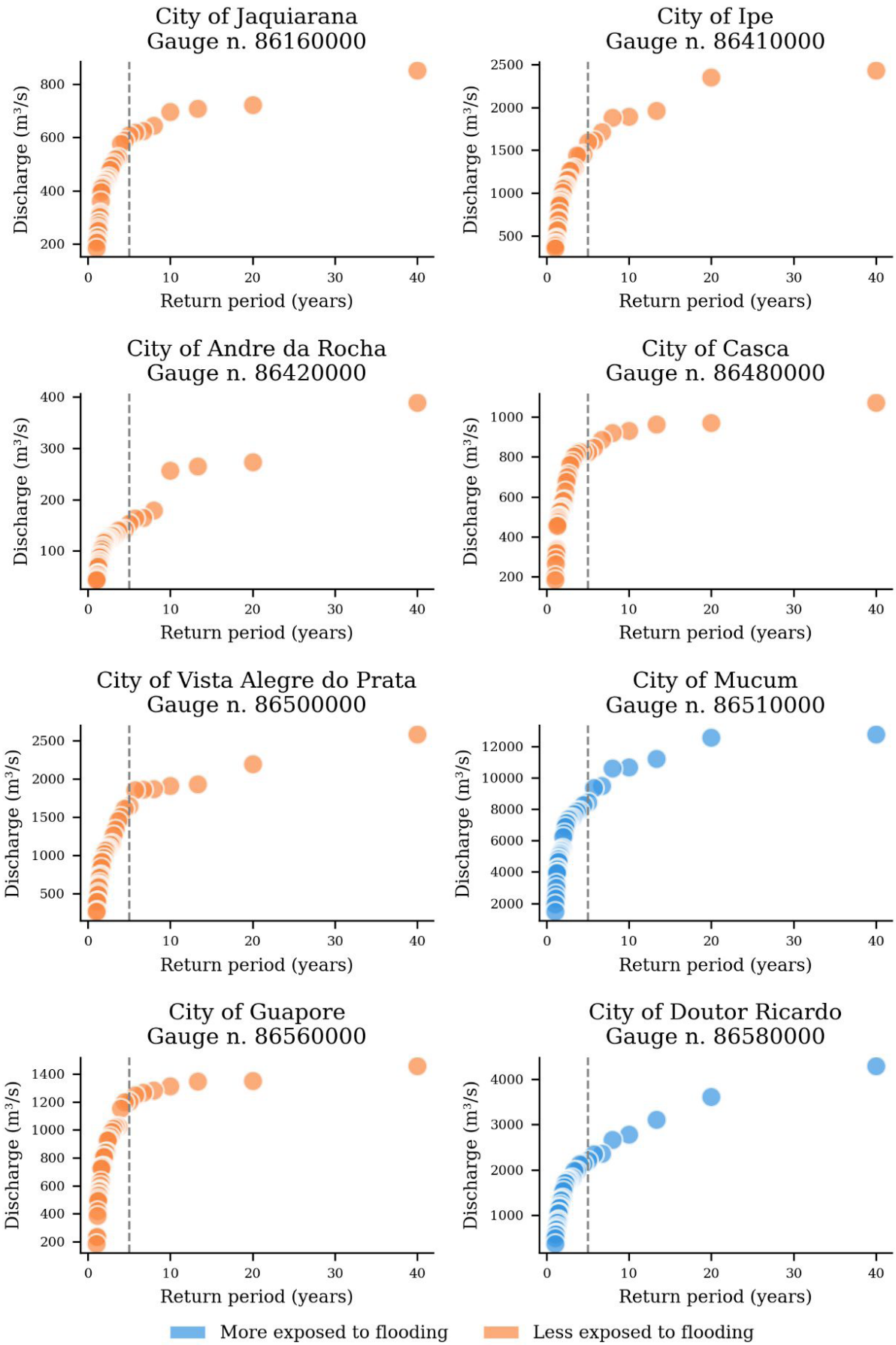

Figure A7. Flood frequency curves for the studied gauge stations, with the dashed line representing RP = 5 years, image 6 of 7.

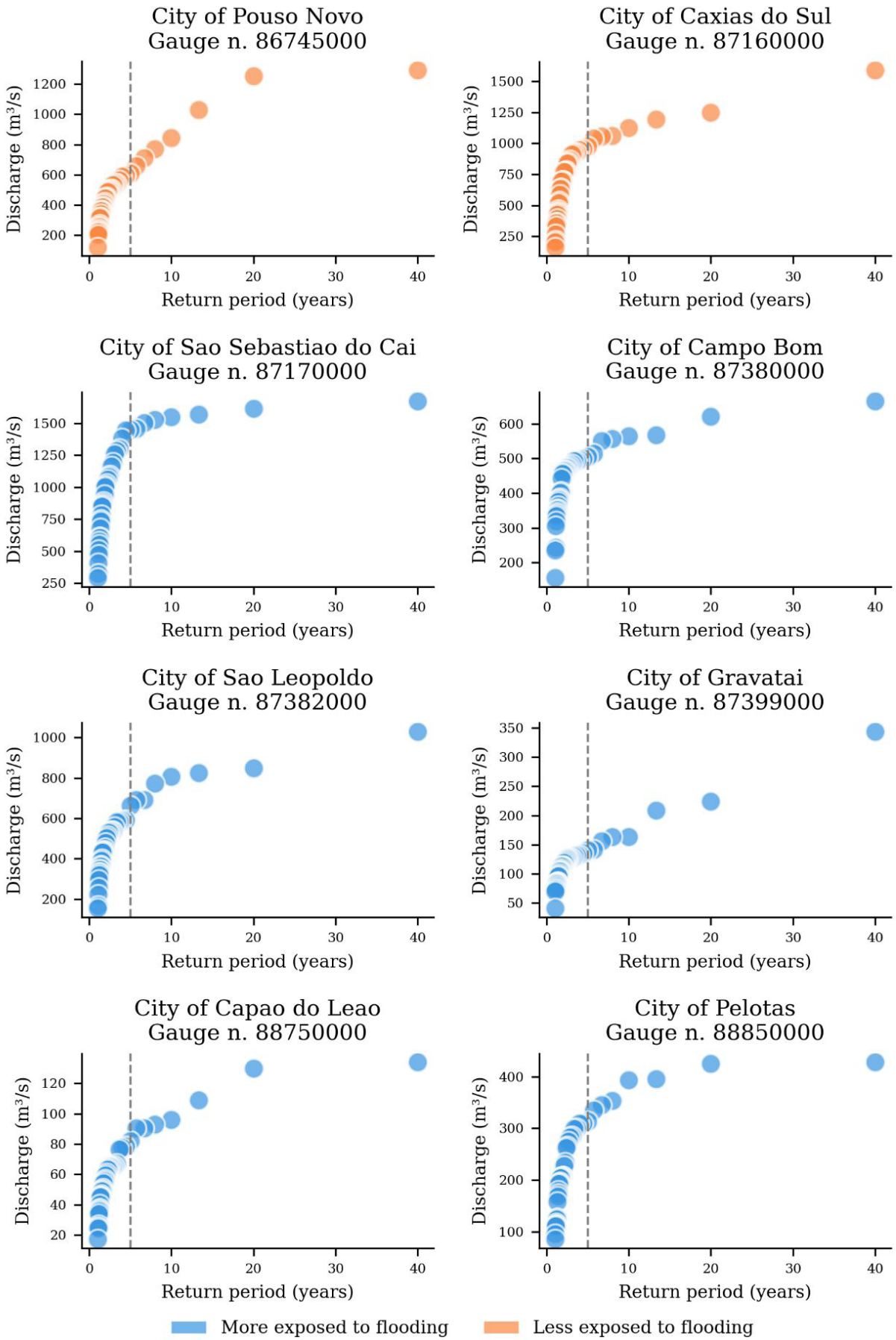

Figure A8. Flood frequency curves for the studied gauge stations, with the dashed line representing RP = 5 years, image 7 of 7.

SUPPLEMENTARY MATERIAL

Supplementary material accompanies this paper.

Supplementary material S1. Data used in the research and calculated morphometric parameters for each gauge station.

This material is available as part of the online article from https://doi.org/10.1590/2318-0331.302520250009.